DOI: 10.1002/chem.200701418

Insights into Sonogashira Cross-Coupling by High-Throughput Kinetics and Descriptor Modeling

Markus R. an der Heiden,[a] Herbert Plenio,*[a] Stefan Immel,[b] Enrico Burello,[c] Gadi Rothenberg,[c] and Huub C. J. Hoefsloot[d]

Abstract: A method is presented for the high-throughput monitoring of reaction kinetics in homogeneous catalysis, running up to 25 coupling reactions in a single reaction vessel. This method is demonstrated and validated on the Sonogashira reaction, analyzing the kinetics for almost 500 coupling reactions. First, one-pot reactions of phenylacetylene with a set of 20 different *meta*- and *para*-substituted aryl bromides were analyzed in the presence of 17 different Pd–phosphine complexes. In addition, the temperature-dependent Sonogashira reactions were examined for 21 different ArX (X = Cl, Br, I) substrates, and the corresponding activation enthalpies and entropies were determined by means of Eyring plots: ArI ($\Delta H^{\ddagger}$ = 48–62 kJ mol^{-1}; $\Delta S^{\ddagger}$ = −71–−39 J mol^{-1} K; $NO_2 \rightarrow OMe$), ArBr ($\Delta H^{\ddagger}$ = 54–82 kJ mol^{-1}, $\Delta S^{\ddagger}$ = −55–11 J mol^{-1} K), and ArCl ($\Delta H^{\ddagger}$ = 95–144 kJ mol^{-1}, $\Delta S^{\ddagger}$ = −6–100 J mol^{-1} K). DFT calculations established a linear correlation of $\Delta H^{\ddagger}$ and the Kohn–Sham HOMO energies of ArX (X = Cl, Br, I) and confirmed their involvement in the rate-limiting step. However, despite different C–X bond energies, aryl iodides and electron-deficient aryl bromides showed similar activation parameters.

Keywords: cross-coupling · homogeneous catalysis · palladium · parallel screening · QSAR · Sonogashira coupling

Introduction

The Sonogashira reaction is used for coupling aryl- and vinyl halides[1–3] or alkyl halides[4] with terminal acetylenes. It is a versatile C–C bond formation reaction that tolerates a variety of functional groups and conditions.[5–22] Sonogashira coupling is applied for producing pharmaceutical intermediates, liquid crystals, polymers, and materials with specialized optical and electronic properties.[23–38] Despite these numerous applications, our mechanistic understanding of the Sonogashira reaction is limited.[39,40] This is because the Sonogashira reaction, like other coupling reactions, has a complex catalytic cycle that involves several steps.[41–47] One approach for unravelling the reaction mechanism is to study the kinetics of the (rate-limiting) elementary steps, such as, oxidative addition,[48] reductive elimination,[49] or transmetalation[50] in detail, all of which, however, need to be known (see Figure 1).[45,51] The widespread belief is that the oxidative addition of the aryl halide determines the turnover for cross-coupling reactions,[52] although Kozuch and Shaik suggested an integrated rate function for the entire catalytic cycle.[53]

Alternatively, one can study the influence of different structural and compositional variables on the outcome of the catalytic reaction, and identify the key factors by statistical analysis. For this, a large and diverse dataset is required. In the case of the palladium-catalyzed Sonogashira reaction, this means a large number of different substituents in the reactants, as well as a variety of ligand–Pd complexes. The problem is that this approach is time-consuming and labor-

[a] Dr. M. R. an der Heiden, Prof. Dr. H. Plenio
Inorganic Chemistry, Zintl-Institute
Darmstadt University of Technology
Petersenstrasse 18, 64287 Darmstadt (Germany)
E-mail: plenio@tu-darmstadt.de

[b] Dr. S. Immel
Organic Chemistry, Schöpf-Institute
Darmstadt University of Technology
Petersenstrasse 18, 64287 Darmstadt (Germany)

[c] Dr. E. Burello, Prof. Dr. G. Rothenberg
van't Hoff Institute of Molecular Sciences
University of Amsterdam
Nieuwe Achtergracht 166, 1018 WV Amsterdam (The Netherlands)

[d] Dr. H. C. J. Hoefsloot
Biosystems Data Analysis, University of Amsterdam
Nieuwe Achtergracht 166, 1018 WV Amsterdam (The Netherlands)

Supporting information for this article is available on the WWW under http://www.chemeurj.org/ or from the author and includes procedures for catalyst preparation; additional tabular material, full listing of activation parameters and data analysis methods; details of computational methods and additional material for the DFT calculations.

 © 2008 Wiley-VCH Verlag GmbH & Co. KGaA, Weinheim

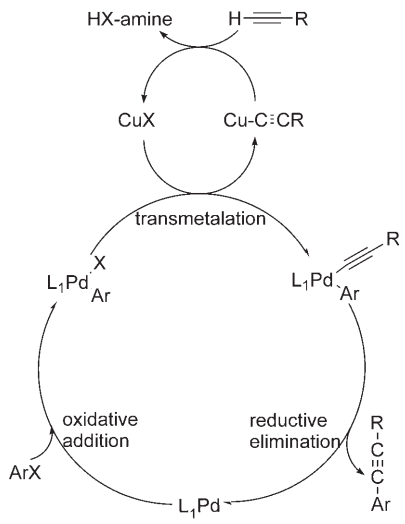

Figure 1. Simplified consensus mechanism for the Sonogashira reaction by using bulky phosphines.

intensive, and therefore unpopular. However, this problem can be solved if reactions are performed in parallel. Kagan and co-workers pioneered a technique termed "one-pot multisubstrate screening",[54,55] in which several reactions with a single catalyst are carried out simultaneously in one reaction vessel to increase the number of substrates studied and to obtain yield and *ee* data much faster. We have modified and extended this method to now make it a reliable technique for the collection of a large amount of kinetic data in homogeneous catalysis. Previously, high-throughput screening (HTS) techniques have been used primarily for speeding up the optimization of Sonogashira catalysts.[21,31,56] Ideally, our approach leads to the identification of a number of quantitative steric and electronic parameters which allow the prediction of the efficiency of a given cross-coupling reaction. Notably, Fairlamb and co-workers have attempted to achieve this by evaluating the electronic properties of the modified dba (dibenzylideneacetone) type of ligands in [Pd_2-$(dba)_3$] and their effect on Suzuki and Heck cross-coupling reactions.[57–59]

Herein, we present a method for high-throughput monitoring of reaction kinetics in homogeneous catalysis.[60–64] We demonstrate and validate this method on the Sonogashira reaction, analyzing the rate constants for almost 500 cross-coupling reactions in three sets. Complementing the high-throughput experimental approach, we then applied DFT calculations and statistical analysis tools, extracting mechanistic information from the data. Importantly, this approach gives an unbiased view of the factors that control the catalytic cycle.

Results and Discussion

Concept validation for Sonogashira cross-coupling: The one-pot multisubstrate screening concept has several key advantages: First and foremost, it is fast. This concerns the actual reactions, as well as their analysis. The time required for the quantitative analysis of the products is drastically reduced, because all products are separated and quantified simultaneously. Moreover, as the reactions are performed simultaneously in the same flask, the conditions are truly identical. This method enables a good sampling of the catalyst and reaction space, and the conclusions are less likely to be biased by the choice of experiments. However, there are also limitations: First, the reactions studied must be selective, as the formation of numerous by-products may impede the quantitative analysis. Fortunately, the Sonogashira reaction is compliant in this respect: The only undesired product resulting from Pd^{2+} ions observed is the Hay coupling product, 1,4-diphenyl-butadiyne, formed with a yield of $<0.3\%$. Second, the rates of individual product formation in each batch should all be within two orders of magnitude.[65] In the case of very fast reactions, approximating the reactant concentration becomes increasingly difficult, whereas in the very slow cases the effective catalyst concentration per substrate does not remain constant once the faster coupling reactions are completed. This is illustrated in Figure 2, which shows the

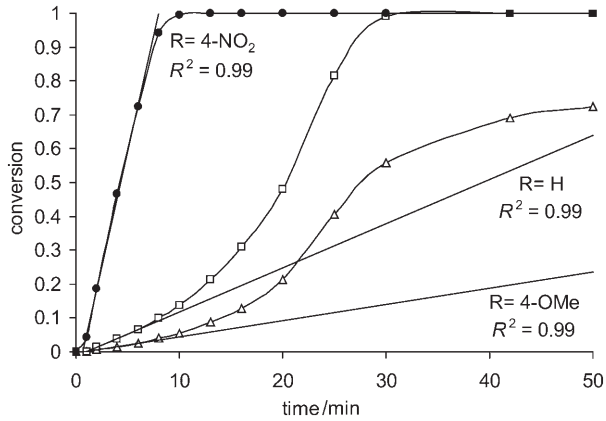

Figure 2. Conversion versus time curves and determination of the initial rates of the product-forming reaction. Subset of data taken from MS-25 screen. "R" symbols denote the *para*-substituent on the aryl bromide, whereas R^2 is the correlation coefficient of the linear fit.

reaction profiles for a subset of three substrates selected from a 25 multisubstrate screen (MS-25). As soon as the fast substrates are converted, the apparent rate for the formation of the "slow" tolanes increases, as more and more catalyst is available for their conversion. Finally, the substituents at the aryl bromides must not react with one another. Considering these limitations, one must first validate the one-pot multisubstrate screening prior to application in the Sonogashira coupling reaction.

Thus, we first studied whether the relative reaction rates (by using standard procedures) match those from the multisubstrate screens. To answer this crucial question, we determined the initial Sonogashira coupling rates for three different substrates (R = −H, −OMe, and $-CO_2Et$, see Table 1) in three individual reaction vessels. Analogous data were then obtained from several multisubstrate screens of various sizes

 © 2008 Wiley-VCH Verlag GmbH & Co. KGaA, Weinheim

Table 1. Verification of the Sonogashira coupling "one-pot multisubstrate screen".[a]

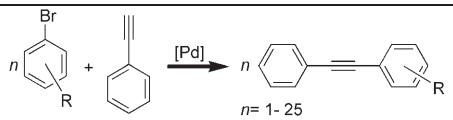

Screen R:	*p*-NO_2	*p*-CN	*p*-COMe	*p*-CO_2Et	*p*-CF_3	*p*-F	H	*p*-Me	*p*-OMe
3×solo	–	–	–	2.07±0.3	–	–	≡1	–	0.6±0.09
MS-2	–	–	–	2.19±0.16	–	–	≡1	–	–
MS-3	–	–	–	2.44±0.18	–	–	≡1	–	0.57±0.04
MS-5	–	–	–	2.49±0.18	2.1±0.16	–	≡1	0.6±0.05	0.59±0.04
MS-9	8.95±0.89	6.35±0.54	3.72±0.26	2.36±0.17	2.13±0.16	0.84±0.05	≡1	0.6±0.05	0.56±0.04
MS-25	9.14±0.91	6.29±0.53	3.9±0.27	2.55±0.19	2.04±0.16	0.83±0.05	≡1	0.61±0.05	0.57±0.04
average	–	–	–	2.35±0.17	2.12±0.16	–	–	0.6±0.05	0.58±0.04

[a] Conditions: $HNiPr_2$, 80 °C, Na_2PdCl_4, CuI, $tBu_3P{\cdot}HBF_4$ = 4:3:4. The remaining 16 R groups in MS-25: *o*-CN, *m*-SOMe, *o*-COMe, *o*-CO_2Et, *p*-SOMe, *m*-COMe, *m*-CF_3, *m*-CO_2Et, *m*-F, *o*-Me, *m*-Me, *o*-OMe, *m*-OMe, *m*-NMe_2, *p*-*t*Bu, *p*-NMe_2.

(MS-2, MS-3, MS-5, MS-9, and MS-25), each carried out in a single reaction vessel. Table 1 lists the relative rates obtained from these experiments (normalized for H≡1). Indeed, we found that the relative rates for a given substrate were all within the experimental error. They were independent of the number of substrates in the multisubstrate screen. This is apparent when comparing various experiments including the aryl bromides with R = *p*-CO_2Et and *p*-OMe, which have been studied in the entire test screens. For *p*-CO_2Et, the deviation from the average of 2.35 is <10%, whereas the deviation of *p*-OMe (average 0.58) is <4%.

We also tested whether a change in the total concentration of the aryl bromide or the phenylacetylene influences the relative rates. In addition to the concentration Σ(ArBr) = 0.1 M for the sum of all aryl bromides used in all experiments, we also studied Σ(ArBr) = 0.2 M. For both multisubstrate experiments (MS-5, RC_6H_4Br; R = $-CF_3$, −H, $-CH_3$, −OMe, −COMe) the relative rates were identical within the experimental error (see the Supporting Information for details). These results validate the one-pot multisubstrate screening for acquiring kinetic data in Sonogashira cross-coupling reactions, and therefore we proceeded with the mechanistic studies.

Ligand and aryl bromide substituent effects: In the first set of reactions (Table 2), we studied the influence of various *meta*- and *para*-substituted aryl bromides and various Pd–phosphine ligand complexes on the Sonogashira reaction rate. In a typical experiment, one equivalent of an equimolar stock solution of mixed aryl bromides **1a**–**1u** (the notation **1l** is omitted to avoid confusion) was stirred in $HNiPr_2$ with 0.001 equivalents (0.1 mol%) of the catalyst complex for ten minutes. The reaction was then initiated by adding 1.05 equivalents of phenylacetylene. The Sonogashira coupling reactions were performed according to a procedure recently described by us; all of the tolanes synthesized for this study have been prepared before and their characterization data reported in detail elsewhere.[12] Reaction progress was monitored by quantitative GC analysis. In total, we measured the initial reaction rate constants for 20 substituted aryl bromides in the presence of 17 different phosphine ligands (nBu_3P, Cy_2PBn, PCy_3, $iPrPCy_2$, iPr_2PCy, iPr_3P, $secBu_3P$, $tBuPiPr_2$, $AdPCy_2$, $tBuPCy_2$, tBu_2PCy, Ad_2PEt, tBu_2PiPr, tBu_3P, tBu_2PBn, Ad_2PtBu, Ad_2PBn) (Ad = 1-adamantyl, Bn = benzyl). All of the phosphines under investigation were trialkylphosphines, the steric bulks of which were modified in a systematic manner. For the Ad_2PR series of phosphines Ad_2PtBu, Ad_2PiPr, Ad_2PBn, Ad_2PEt, the size of the R group was modified. With the butyl series nBu_3P, $secBu_3P$, and tBu_3P, the degree of branching was modified and, within the R_2PBn series Cy_2PBn, tBu_2PBn, Ad_2PBn, the nature of R was varied. Within the series PCy_3, $tBuPCy_2$, tBu_2PCy, tBu_3P, the cyclohexyl groups were replaced by *t*Bu groups. The steric bulk was expected to increase in a steady manner. However, the sum reactivities of

Table 2. Sonogashira cross-coupling reactions of 20 different aryl bromides in the (20×1) screen with the various Pd-phosphine catalysts as defined by the respective 17 phosphines. Phosphine used: Ad_2PBn; $AdPCy_2$; tBu_2PBn; Ad_2PtBu; Ad_2PEt; $PtBu_3$; $PsecBu_3$; nBu_3; tBu_2PiPr; Cy_2PBn; $PiPr_3$; PCy_3; Cy_2PtBu; $CyPtBu_2$; Cy_2PiPr; iPr_2PtBu; iPr_2PCy.

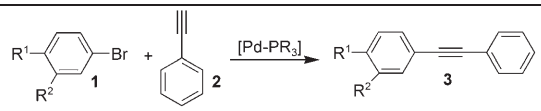

Aryl bromide	Tolane	R^1	R^2
1a	**3a**	H	H
1b	**3b**	CF_3	H
1c	**3c**	F	H
1d	**3d**	Me	H
1e	**3e**	OMe	H
1f	**3f**	CN	H
1g	**3g**	*t*Bu	H
1h	**3h**	COMe	H
1i	**3i**	NO_2	H
1j	**3j**	CO_2Et	H
1k	**3k**	NMe_2	H
1m	**3m**	S(O)Me	H
1n	**3n**	H	CF_3
1o	**3o**	H	F
1p	**3p**	H	Me
1q	**3q**	H	OMe
1r	**3r**	H	Ac
1s	**3s**	H	NMe_2
1t	**3t**	H	CO_2Et
1u	**3u**	H	S(O)Me

 © 2008 Wiley-VCH Verlag GmbH & Co. KGaA, Weinheim

the respective Pd-complexes ($SR_i = 0.078$, 0.48, 0.52, 1.00), see Table 3) did not show the expected smooth increase in activity. PCy_3 is poor, but beyond a critical threshold of steric bulk, represented by tBuPCy$_2$, the catalytic activity did not change drastically.[66] From this observation, as well as from the analysis of the remaining series of phosphines we concluded that highly active catalysts require at least one tertiary and two secondary carbon atoms attached to the phosphorus atom for good activity. As soon as two tertiary carbon atoms are present, the third substituent on the phosphorus atom can be almost any group without compromising very high activity catalysts. This may explain why some groups showed excellent catalytic activities with Pd-phosphine complexes of the latter type, for example, tBu$_2$PMe,[67] Ad$_2$PnBu,[68] and tBu$_2$POH.[69] This yielded a set of 340 reaction profiles with 340 corresponding rate constant (k_{obs}) values. Figure 3 shows the entire set of rate constants for the various substrate/ligand combinations.

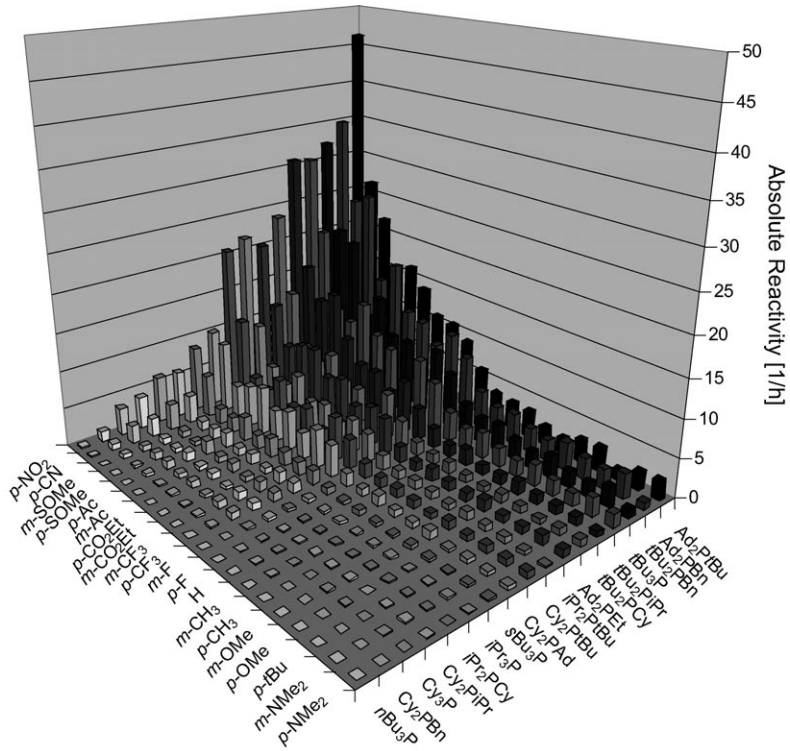

Figure 3. Rate constant (reactivity 1000 h^{-1}) for 340 Sonogashira reactions of 20 aryl bromides with phenylacetylene, applying 17 different Pd–phosphine complexes. Solvent: HNiPr$_2$, $T = 80$ °C; catalyst: Na$_2$PdCl$_4$, CuI, phosphonium salt: 4:3:4. Reactivities are low-conversion tof.

Table 3. Sum reactivities SR_i, reaction constants ρ and σ_p^- correlation coefficient (R^2 (σ^0_{para}) for comparison only) for all reactions at 80 °C.[a]

Phosphine	SR_i	ρ(para)	$R^2(\sigma^-_{para})$	$R^2(\sigma^0_{para})$
Cy$_2$PBn	0.031	0.948	0.931	0.894
PCy$_3$	0.078	1.057	0.969	0.888
iPrPCy$_2$	0.085	1.018	0.951	0.860
iPr$_2$PCy	0.10	1.123	0.905	0.823
iPr$_3$P	0.13	1.038	0.935	0.932
secBu$_3$P	0.18	0.975	0.977	0.863
tBuPiPr$_2$	0.44	0.991	0.918	0.917
AdPCy$_2$	0.45	0.891	0.939	0.859
tBuPCy$_2$	0.48	0.893	0.973	0.791
tBu$_2$PCy	0.52	0.921	0.972	0.762
Ad$_2$PEt	0.56	0.931	0.989	0.822
tBu$_2$PiPr	0.72	0.963	0.923	0.842
tBu$_3$P	1.00	0.790	0.970	0.828
tBu$_2$PBn	1.07	0.813	0.928	0.909
Ad$_2$PtBu	1.26	0.821	0.930	0.728
Ad$_2$PBn	1.33	0.834	0.960	0.866

[a] The sum reactivity SR_i is defined by Equation (1).

$$SR_i = \frac{1}{n_{substrate}} \cdot \sum_{i=1}^{n} \frac{r_{R_i\,ArX}(PR_3)}{r_{R_i\,ArX}(t\mathrm{Bu}_3\mathrm{P})} \quad (1)$$

Phosphine ligand steric effects: The ligand size influences the catalytic activity of the Pd catalyst complexes. In general, the empirical rule that sterically demanding and electron-rich phosphines yield high activity catalysts is confirmed.[70] We find, for example, that Pd–PCy$_3$ is a relatively poor catalyst, whereas Pd–tBu$_3$P is 10–50 times more active in the conversion of aryl bromides at 80 °C. However, describing the ligand effects by using only the Tolman cone angles[71] is insufficient. Modeling the entire sum of the reactivities' dataset by using Tolman's cone angles gives a poor correlation, even when excluding the P(nBu)$_3$ ligand that is distant from the line ($R^2 = 0.44$ for 17 observations). This may reflect fundamental problems of the Tolman approach especially concerning PR$_3$ ligands with different R groups.[72–74] However, it is likely that in this case the activity does not depend only on steric effects, but rather on a combination of steric, electronic, and interaction effects (see below). We can isolate the steric effect for some of the ligands, for example, for the subset {P(iPr)$_3$; P(secBu)$_3$; P(iPr)$_2t$Bu; PiPr(tBu)$_2$; P(tBu)$_3$; P(1-Ad)$_2t$Bu}. The correlation coefficient for this subset is $R^2 = 0.993$ for six observations (Figure 4). In this subset, the iPr residues are substituted either with 1-Ad or with tBu groups. These are both aliphatic anchor groups with spherical symmetry (as opposed to Bn or Cy).

Descriptor modeling and Hammett parameters: High-throughput experiments as described here yield large amounts of data with high precision and reproducibility. Ex-

 © 2008 Wiley-VCH Verlag GmbH & Co. KGaA, Weinheim

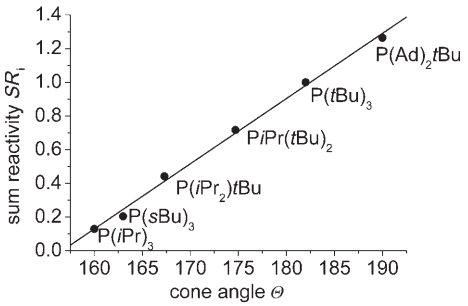

Figure 4. Reactivity versus cone angle for six phosphine ligands, substituting *i*Pr groups with *t*Bu or 1-Ad groups.

tracting useful information from this data is a complex problem in itself. We approached the data analysis from two directions, namely using 'blind' statistical models ('black models') that employ no chemical knowledge, as well as descriptor models based on physical organic chemistry. Starting with the raw data, we modeled the rows and columns separately with average value models, using the σ^- and the cone angle parameters. The σ^- parameter (σ for the *meta*-substituents) gives a very good model for the substituent effect, with $R^2=0.930$ for 16 observations (data given in Table 3). In each case, the substituent values for the different ligands are nicely clustered together (data not shown for clarity) so the average gives a good representation of the data spread.

Next we ran a 'blind model' (i.e., a data-driven statistical model), to see whether there are single effects or interaction effects between the ligands and the substituents. In this model, the entire dataset is represented by Equation (2),

$$k_{ij} = C + \tilde{x}_i + \tilde{y}_j + \beta\tilde{x}_i\tilde{y}_j \qquad (2)$$

where C is the overall mean (4.15 h^{-1}), $\tilde{x}_i$ and $\tilde{y}_j$ denote the total-mean-centered values of row i and column j, respectively, and β is an interaction parameter. Using a goal-seek function,[75] we found that $\beta=0.22$ yields a fit of $R^2=0.978$ for all k values (323 observations). This shows that there is a substituent effect, a ligand effect, and an interaction effect. The interaction effect between the ligand and the substituent is important. If we omit the interaction parameter, $R^2=0.803$. Thus, the interaction parameter explains almost 20% of the variance in the data. It is unlikely that the substituent has a steric effect, and even more unlikely that an electronic substituent effect will interact with a steric ligand effect. Thus, we observe here an interaction between a ligand electronic effect and a substituent electronic effect. The Hammett σ^- parameter[76,77] is an excellent descriptor in this case. Note, however, that the literature contains diverse reports: Similar correlations were reported for Suzuki,[78–80] Heck,[81–85] and carbonylation reactions[86] even though *different* Hammett parameters were used: Milstein and Herrmann reported that σ_p^- parameters yielded the best fits, whereas other studies applied σ_p parameters. Even a σ_p^+ correlation to establish a stabilization of a positive charge in the transition state was reported.[81] To further understand the mechanism, we studied the correlations of the reaction rates, relative to R = H, by using also the σ_p^0, σ_p^+, and σ_{meta} parameters.[76] The correlation coefficients of the σ_p^0 were not as good as those for σ_p^- (Table 3). To distinguish between σ_p^0 and σ_p^- correlations, one must study a number of different substituents covering a large range of electronic effects. NMe_2 is especially important in this respect.[76] As expected, σ_p^+ gave poor correlation coefficients. The data for tBu$_3$P with R^2 (σ_{para}^0) = 0.83 versus R^2 (σ_{para}^-) = 0.97 illustrate this point (Figure 5). In contrast to the excellent correlations in the *para* series, the *meta* Hammett parameters produce linear fits with lower correlation coefficients ($R^2=0.7$–0.8). We believe that this reflects the limited value of *meta* Hammett parameters, as noted by Hansch et al.[76]

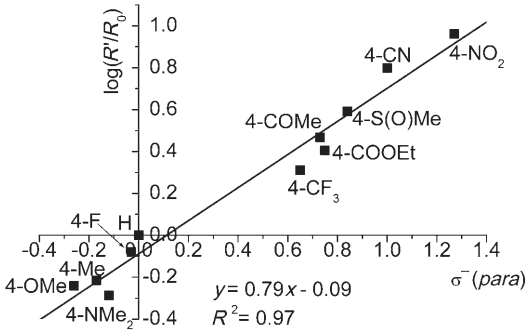

Figure 5. One of the 17 Hammett plots determined for the rates of tBu$_3$P-based Pd-catalyst for the Sonogashira coupling of various 4-substituted aryl bromides (R = NMe_2, Me, OMe, H, F, CF_3, CO_2Et, COMe, S(O)Me, CN, NO_2). R' = reaction rate for variable substituent, R_0 = reaction rate for reference substituent H.

We also correlated the sum reactivity (SR_i) of a given catalyst with the ρ values obtained from the slope of the linear fit of relative reactivity versus the respective Hammett constant. The data cluster in three distinct areas. First of all, the Pd–PR_3 complexes of low activity (Cy_2PBn, PCy_3, iPrPCy$_2$, iPr$_2$PCy, iPr$_3$P, secBu$_3$P)[87] give SR_i $\rho=0.95$–1.12, the second group of intermediate activity represented by the phosphines (AdPCy$_2$, tBu$_2$PCy, tBuPiPr$_2$ Cy$_2$PBn, tBuPCy$_2$, Ad$_2$PEt) are characterized by $\rho=0.89$–0.99, and finally, the high activity phosphines (Ad$_2$PBn, tBu$_3$P, Ad$_2$PtBu, tBu$_2$PBn) by $\rho=0.79$–0.83.

The large ρ values for catalysts of low reactivity explain that substituents at the aryl bromides strongly influence the overall reactivity. This effect is less pronounced for catalysts of intermediate activity and even smaller for those of high activity. The lower sensitivity of high activity catalysts towards the 4-substituents means that all elementary steps that depend on this substituent are less important for the overall rate. This includes the oxidative addition step. Significant changes in ρ indicate a change in the mechanism. It is likely that catalytic reactions in each of the three clusters occur through slightly different mechanisms. Jutand and coworkers noted that depending on the bulk of the phosphine,

 © 2008 Wiley-VCH Verlag GmbH & Co. KGaA, Weinheim

the oxidative addition can occur through an associative or a dissociative mechanism, in agreement with the different ρ values we observe here.[88]

Using a smaller set of data, we also studied the substituent effects in the Sonogashira coupling of aryl iodides and aryl chlorides by using tBu$_3$P-based Pd-catalysts. For both classes of compounds, σ^-_{para} gives better correlation coefficients than σ^o_{para}. However, with aryl chlorides the differences of R^2 between the σ^-_{para} and the σ^o_{para} fit are small. We attribute this ambiguity to the smaller number of different substrates (−NMe$_2$ omitted) studied in the temperature-dependent reaction and not to a change in the correlation pattern. The increasing bond strength C−X results in an increase in the ρ values along the series of aryl chlorides (ρ = 1.3, 80 °C) > aryl bromides (ρ = 0.51, 80 °C; 0.76, 50 °C) > aryl iodides (ρ = 0.38, 50 °C, see Table 4). The oxidative addition rate slows down for stronger C−X bonds, becoming increasingly important for the overall rate equation.

Table 4. Temperature-variable Hammett plots for the Sonogashira reaction of aryl iodides, bromides, and chlorides with phenylacetylene, by using the tBu$_3$P-derived catalyst (R = see Figures 6 and 7).

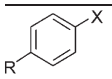

X	T [°C]	$\rho(\sigma^-_{para})$	R^2
I	23.4	0.457	0.97
I	30	0.461	0.98
I	35	0.459	0.99
I	40	0.445	0.97
I	45	0.408	0.97
I	50	0.376	0.98
Br	40	0.921	0.95
Br	50	0.762	0.96
Br	60	0.675	0.95
Br	70	0.568	0.93
Br	80	0.508	0.89
Cl	80	1.336	0.98
Cl	95	1.097	0.95
Cl	108	0.98	0.90

Nonetheless, the large differences in the C−X bond energies (in C$_6$H$_5$−X; X = Cl 402, Br 337, I 272 kJ mol^{-1})[89] do not translate into correspondingly large differences of rates for the Sonogashira coupling reactions. At 50 °C the mean ratio of k_{ArI}/k_{ArBr} is about ten, whereas, at 80 °C, k_{ArBr}/k_{ArCl} reaches about 10000. This is much less than what could be expected on the basis of the mean bond energy differences. Hartwig noted that, with the exception of aryl chlorides, the rate-limiting step is not the actual insertion of the palladium(0) into the C−X bond, but rather the reorganization of the ligand sphere preceding this step.[90]

Temperature effects: To determine the activation parameters $\Delta H^{\neq}$ and $\Delta S^{\neq}$ for Sonogashira coupling we have performed the multisubstrate coupling reactions of various aryl halides 4-R-C$_6$H$_4$-X (X = I, Br, Cl, R: NO$_2$, CO$_2$Et, CF$_3$, H, F, Me, OMe) with phenylacetylene at several different temperatures. The resulting Eyring plots allow the calculation of the activation parameters for all of the 21 coupling reactions (Figures 6 and 7). It should be kept in mind that our data come from the analysis of the whole reaction and not from individual elementary steps.

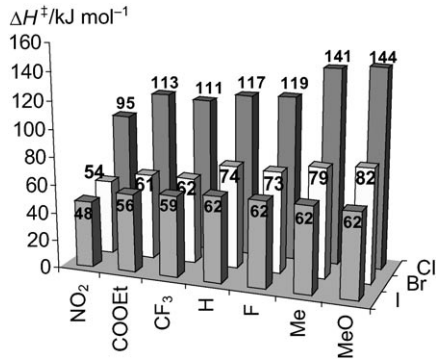

Figure 6. Enthalpies of activation $\Delta H^{\neq}$ for the Sonogashira reactions of 4-R-C$_6$H$_4$-X and phenylacetylene by using a tBu$_3$P-derived Pd catalyst.

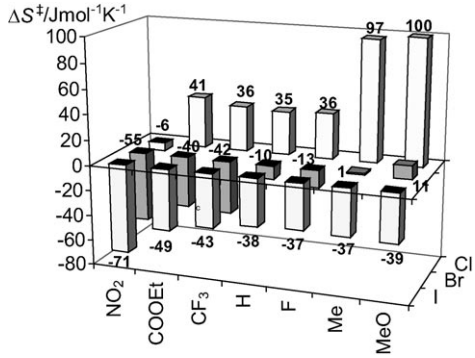

Figure 7. Entropies of activation $\Delta S^{\neq}$ for the Sonogashira reactions of 4-R-C$_6$H$_4$-X and phenylacetylene by using a tBu$_3$P-derived Pd catalyst.

The enthalpies of activation $\Delta H^{\neq}$ are always positive. There is, however, little change (14 kJ mol^{-1}) in the series of ArI (48 → 62 kJ mol^{-1}), slightly more differentiation (28 kJ mol^{-1}) with ArBr (54 → 82 kJ mol^{-1}) and, by far, the biggest change (50 kJ mol^{-1}) with ArCl (94 → 144 kJ mol^{-1}). This indicates the increasing importance of the oxidative addition step for the overall rate.

The entropies of activation provide information on the degree of order in the transition state. It is interesting to observe large differences in the series of ArX (X = Cl, Br, I). The large, negative values for ArI (−71 → −37 J mol^{-1} K) are indicative of a highly ordered transition state corresponding to an associative mechanism. Again the spread of the $\Delta S^{\neq}$ values is larger for the ArBr reaction (−55 → 10 J mol^{-1} K). Although the highly activated aryl bromides show values similar to those of aryl iodides, this changes drastically for the deactivated aryl bromides. With the exception of the nitro-substituted species, the entropies of activation for the aryl chlorides are large and positive (−6 → 100 J mol^{-1} K). Again aryl chlorides and the nonactivated aryl bromides behave distinctly differently from the aryl iodides and the

 © 2008 Wiley-VCH Verlag GmbH & Co. KGaA, Weinheim

activated aryl bromides, the activation parameters of which ($\Delta H^{\ddagger}$ and $\Delta S^{\ddagger}$) are similar. This is true, even though the C–I and C–Br binding energies differ significantly. We conclude that the insertion of Pd into the C–X bond can hardly be rate limiting in the Sonogashira coupling of aryl iodides and activated aryl bromides.

The activation parameters for the oxidative addition of chlorobenzene to Pd(dppe) were determined by Milstein and Portnoy as $\Delta H^{\ddagger} = 118\ \mathrm{kJ\,mol^{-1}}$ and $\Delta S^{\ddagger} = -9\ \mathrm{J\,mol^{-1}\,K}$ ($\pm 33\ \mathrm{J\,mol^{-1}\,K}$).[91] These values agree remarkably well with the activation parameter determined by us for the Sonogashira cross-coupling of chlorobenzene (Figures 6 and 7). Despite this excellent correlation, one should remember that activation parameters can vary, depending on the ring size of the chelating phosphines.[92] Nonetheless, this is strong evidence for the oxidative addition being the rate-limiting step in the Sonogashira coupling of aryl chlorides.

We are not aware of experimental activation parameters for the oxidative addition of aryl bromides to palladium(0).[93,94] Fu and co-workers determined activation parameters for the corresponding reactions of alkyl bromides ($\Delta H^{\ddagger} = 10\ \mathrm{kJ\,mol^{-1}}$) that are significantly smaller than our values for the aryl bromides.[95] Note that our values of $\Delta H^{\ddagger}$ and $\Delta S^{\ddagger}$ for the Sonogashira coupling are different from the $\Delta H^{\ddagger} = 69\ \mathrm{kJ\,mol^{-1}}$ and $\Delta S^{\ddagger} = -43\ \mathrm{J\,mol^{-1}\,K}$ as determined for the Heck coupling of acrylates.[96–98] This comes as no surprise as the cleavage of the much weaker C–I bond during the Heck reaction will be less significant for the overall rate of the catalytic cycle than the oxidative addition of the C–Cl bond. Consequently, the overall activation barrier can hardly be similar for aryl iodide Heck and the Sonogashira coupling reactions. One step within the series of elementary steps comprising the oxidative addition is the actual C–X bond scission,[99] which can only be rate limiting when the respective bond energies correlate with $\Delta H^{\ddagger}$.

Concept validation of the temperature-variable high-throughput screening: To firmly establish the method of parallel multisubstrate screening for the determination of activation parameters, we performed extensive control experiments.

First of all we repeated the multisubstrate experiments by using a set of five 4-substituted aryl bromides (4-R = COMe, CF_3, H, Me, OMe) which were simultaneously reacted with phenylacetylene in an MS-5 experiment at temperatures of 30, 40, 50, 60, 70, and 80 °C. Each experiment was repeated four times (MS-A, -B, -C, -D). The $\Delta H^{\ddagger}$ values thus obtained (Tables 5 and 6) are virtually identical to the $\Delta H^{\ddagger}$ values determined in the MS-7 experiment described above (Figures 6 and 7). This emphasizes the excellent reproducibility and reliability of the parallel multisubstrate screening approach. Next the more important question of whether the multisubstrate approach is able to provide us with meaningful activation parameters must be answered. We have therefore individually determined the activation parameters for each of the five coupling reactions described above. The five different aryl bromides were reacted separately with phenylacetylene at six temperatures between 30–80 °C. Each reaction was repeated four times and we thus studied a total of 180 coupling reactions. The activation enthalpies determined are listed in Table 5. The most important conclusion is that $\Delta H^{\ddagger}$ and $\Delta S^{\ddagger}$, which are values determined in single reaction experiments (solo), are identical (within the error of the experiment) to those determined in the multisubstrate (MS-5) experiment. These experiments unequivocally prove that parallel multisubstrate screening is a viable and efficient method for the study of cross-coupling reactions.

Table 5. Activation enthalpies $\Delta H^{\ddagger}$ obtained from parallel multisubstrate experiments. Each experiment was repeated four times (columns A, B, C, and D); the fifth column is the average.

	MS-A [kJ mol^{-1}]	MS-B [kJ mol^{-1}]	MS-C [kJ mol^{-1}]	MS-D [kJ mol^{-1}]	Average [kJ mol^{-1}]
COMe	52.7 ± 4.1	53.5 ± 4.1	53.0 ± 4.1	52.3 ± 4	52.8 ± 4.1
CF_3	61.6 ± 4.4	62.0 ± 4.5	60.8 ± 4.4	60.6 ± 4.4	61.2 ± 4.4
H	72.9 ± 2.6	72.9 ± 2.6	72.2 ± 2.5	72.7 ± 2.5	72.7 ± 2.5
Me	80.7 ± 5.6	80.0 ± 5.5	80.4 ± 5.5	80.8 ± 5.6	80.5 ± 5.6
OMe	82.2 ± 6.4	84.0 ± 6.6	83.0 ± 6.5	83.1 ± 6.5	83.1 ± 6.5

Table 6. Activation enthalpies $\Delta H^{\ddagger}$ obtained from single reaction experiments. Each experiment was repeated four times (columns A, B, C, and D); the fifth column is the average.

	Solo-A [kJ mol^{-1}]	Solo-B [kJ mol^{-1}]	Solo-C [kJ mol^{-1}]	Solo-D [kJ mol^{-1}]	Average [kJ mol^{-1}]
COMe	50.2 ± 4.4	52.2 ± 4.6	53.6 ± 4.7	52.4 ± 4.6	52.1 ± 4.6
CF_3	61.4 ± 2.5	61.8 ± 2.5	62.3 ± 2.6	62.3 ± 2.6	62.0 ± 2.5
H	72.6 ± 2.3	72.3 ± 2.3	72.4 ± 2.3	72.3 ± 2.3	72.4 ± 2.3
Me	82.1 ± 6.8	81.8 ± 6.8	81.7 ± 6.8	81.4 ± 6.8	81.8 ± 6.8
OMe	84.9 ± 6.6	84.0 ± 6.6	83.8 ± 6.5	83.3 ± 6.5	84.1 ± 6.6

DFT calculations on aryl halide substrates: Scheme 1 outlines two different isodesmic reactions, both of which have been used previously to evaluate the stability of poly(chlorobenzene)s.[100] We used these for evaluating the stability of the C–X bond. Although the closed-shell reaction of type I describes well the electronic situation of the oxidative addition to palladium(0), the radical type II reaction was included for comparison (see Supporting Information). We consider the closed-shell reaction of type I as the more realistic

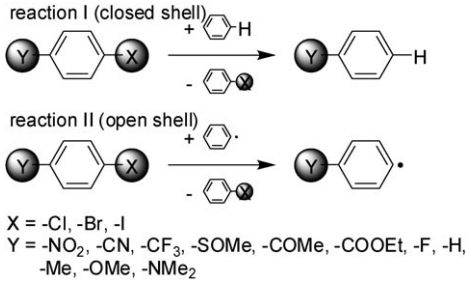

Scheme 1. Isodesmic reactions type I and II for evaluating substituent effects on aryl-halogen bond energies of various *para*-substituted (Y) halogen benzenes (X) relative to their unsubstituted counterparts (Y = H).

 © 2008 Wiley-VCH Verlag GmbH & Co. KGaA, Weinheim

model, as the C–X scission in cross-coupling reactions is probably not a free-radical process.[101]

In fact, there is no distinct and significant correlation between the calculated C–X bond strength that is, the ΔH or ΔG values (as determined through B3LYP/6-311++G-(d,p)[102–107] with the halogen atoms Cl, Br, and I represented by Los Alamos LanL2DZ[108] effective core potentials, ECP) from the isodesmic reactions of type I and II and the relative rate constants ($\log_{10} k_{RY/RH}$) obtained for the Sonogashira reaction of the series of substituted aryl halides under consideration. Based on this we believe that the actual breaking of the C–X bond, that is, the insertion of palladium(0), is not rate-limiting.[109] With a view to the arbitrary choice of the reference state for the C–X bond strength, we looked into other molecular parameters that could shed some light on the role of the Sonogashira substrates in the mechanism of the reaction.

The DFT-derived energies of the Kohn–Sham molecular orbitals (B3LYP/6-311++G(d,p)) are good descriptors in this case. Both the HOMO and the LUMO energies are related to the Hammett σ reaction parameters, although only the HOMO energies (E_{HOMO}) exhibit an almost linear correlation. An ostensive relationship between $\Delta H^{\neq}$ and E_{HOMO} is shown in Figure 8. This correlation suggests that the aryl halides participate in the turnover-determining step of the Sonogashira reaction. Presumably, this step is preceded by an end-on ligation of the halogen atom to the Pd atom, and therefore can be regarded as an electron-donating step.[99] The higher the E_{HOMO} of the substrate, the more stable this pre-complex should be, and the higher the rate-determining activation barrier for subsequent steps. Thus, p-NMe_2-substitution makes the aryl halide a better ligand (high E_{HOMO}), whereas the p-NO_2 lowers the E_{HOMO}, facilitating the ensuing oxidative addition reaction. Although these effects are most pronounced for the aryl chlorides, they decrease in the order X = Cl > Br > I. Specifically, the correlation of an intrinsic property of the aryl halide with $\Delta H^{\neq}$ means that significant steps influencing the overall rate must occur whilst the aryl halides exist within the catalytic cycle (before the insertion of palladium(0) into the C–X bond).

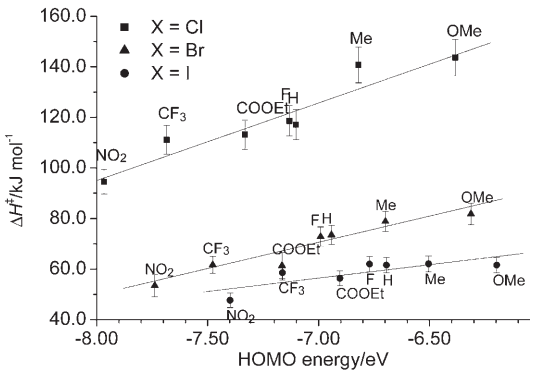

Figure 8. Plot of experimental enthalpies of activation $\Delta H^{\neq}$ against calculated Kohn–Sham HOMO energies for the series of substituted R-C_6H_4-X. The regression coefficient (R^2) values are 0.95, 0.96, and 0.90 for X = Cl, Br, and I, respectively.

Conclusion

Parallel multisubstrate screening is a valid experimental method for studying Sonogashira cross-coupling reactions and to establish structure–activity relationships. This approach will allow understanding of the factors which control the outcome of Sonogashira reactions and ideally lead to a set of steric and electronic parameters which govern such coupling reactions. Ideally, this will allow prediction of the rate at which coupling reactions occur. The ease and speed of this approach enable the quantification of hundreds of reaction profiles in a few weeks. The simultaneous screening under identical conditions gives additional advantages, such as the possibility of applying statistical models to the data and extracting relevant mechanistic information. Moreover, extensive verification experiments carried out for this study provide firm concept validation.

Specifically, the Hammett correlations by using σ^{-}_{para} for 17 sets of Sonogashira reactions demonstrate the stabilization of a negatively charged transition state for the coupling reactions of all aryl halides (X = Cl, Br, I). For all 17 catalysts a correlation of the sum reactivity SR_i and ρ clusters the data in three distinct areas: Low cone angle/poor activity catalysts result in large ρ values, intermediate cone angle and activity give medium ρ values, and high cone angle and activity gives small ρ values. For unbranched phosphines the cone angle is correlated with the reactivity of the respective Pd catalysts. The role of the aryl halide is emphasized by DFT calculations, which link the Kohn–Sham HOMO energy of the aryl halide with the activation enthalpy. The correlation of the HOMO energy of the various substituted aryl halides (X = Cl, Br, I) with activation enthalpy $\Delta H^{\neq}$ for all of the 21 different aryl halides shows that the aryl halide has to be involved in the rate-limiting step. We have demonstrated parallel multisubstrate screening to be useful to understand coupling reactions; the parameterization of substituent and ligand effects is desirable to gain predictive character.

Experimental Section

Gas chromatography: Two Perkin–Elmer gas chromatographs were used: A GC Autosystem for manual injection equipped with a split/splitless injector system and a FID detector. A Clarus 500 GC with an autosampler and equipped with a split/splitless injector system and a FID detector. Chromatographic separation on both GC instruments was performed by using a 15 m × 0.25 mm, df 1.0 μm Varian CP-Sil 8 CB column. Nitrogen was used as carrier gas at flow rates between 0.3 and 0.4 mL min^{-1} and helium with a programmed velocity of 25 cm s^{-1}, respectively. For HETP (height equivalent of a theoretical plate) experiments also H_2 and Ar were used as carrier gas at different flow rates between 0.25 and 1.2 mL min^{-1}. All the injections were made in the split flow mode with a split ratio of either 20:1 or 50:1. For all analyses, the injector was maintained at 270 °C and the detector at a temperature of 350 °C. Signal acquisition and data handling was performed by using the IntLink Clarus data acquisition system and TotalChrome V6.3 Workstation (Perkin–Elmer Inc., Shelton, Connecticut, USA). Quantification of the components was accomplished by using two internal standards (dibenzofurane and naphthalene) for screening experiments with GC separation runtimes

 © 2008 Wiley-VCH Verlag GmbH & Co. KGaA, Weinheim

greater than 45 min and by using one internal standard (dibenzofurane) with faster runtimes. The concentration of the standards was the same as for each of the substrates in the reaction ($0.1/n_{components\ M}$). Calibration was performed with substrate/standard- and product/standard-ratio stock solutions in the range of 1:1000 to 1:1 to obtain the calibration curves for the respective GC system and detector. The concentrations of the calibration levels were according to screening conditions 0.1 mol L^{-1} for the sum of all components. A sample was taken at full conversion in all screening experiments to approve calibration precision and trueness under screening conditions. The validation process of the GC-FID and GC-MS methods was performed according standard procedures[110] and EURACHEM guidelines. The methods were validated in terms of limit of detection (LOD), limit of quantification (LOQ), linearity, precision, and trueness

Ready-made Sonogashira catalyst:[12] All of the catalyst components (CuI, Na_2PdCl_4, and $(tBu)_3P{\cdot}HBF_4$) were mixed together and finely ground with the inert salt $HNiPr_2{\cdot}HBr$. This mixture was used for all screening experiments in which the reactivity of the substrates was the key point of interest. The intention behind this procedure was the better comparability combined with a small error in the Pd/Cu/P ratio. A mixture of CuI (14.3 mg, 75 μmol) Na_2PdCl_4 (29.4 mg, 100 μmol) and phosphonium salt $(tBu)_3P{\cdot}HBF_4$ (58.3 mg, 201 μmol) was finely ground with the inert salt $HNiPr_2{\cdot}HBr$ (1898 mg). The molar ratio of Pd/Cu/P was 4:3:8 and the use of 20.0 mg of this mixture for a coupling reaction with 1 mmol of aryl halide equals a TON of 1000 at full conversion.

Separate-component catalyst: Each of the components (Na_2PdCl_4; CuI; phosphine) were dispersed separately in $HNiPr_2{\cdot}HBr$ and were weighed together before starting the coupling reactions. Part A (palladium composition): Na_2PdCl_4 (26.4 mg, 89.8 μmol) was finely ground with the inert salt $HNiPr_2{\cdot}HBr$ (420.0 mg). Part B (copper composition): CuI (14.8 mg, 77.7 μmol) was finely ground with the inert salt $HNiPr_2{\cdot}HBr$ (504.6 mg). Part C (phosphine composition): The respective phosphine (89.8 μmol) was finely ground with the inert salt $HNiPr_2{\cdot}HBr$.

Stock solutions: For better comparability of the screening experiments different stock solutions were prepared. Different aryl halides or acetylenes were weighed with the appropriate amount of the internal GC standard and then filled up with $HNiPr_2$ to reach the required concentration. The solution was then siphoned into a Schlenk tube and was carefully degassed by freeze and thaw cycles. The final concentration for the aryl halide stock solutions was 1 M for the sum of all components and (n(components) M)$^{-1}$ for each of the internal GC standards (dibenzofurane and naphthalene). The final concentration for the phenylacetylene stock solutions was 0.5 M for the sum of all components and also 0.5/n components M for the internal GC standards.

Procedures for the Sonogashira coupling of aryl bromides and acetylenes: preparation of the GC standards: A mixture of the ready-made Sonogashira catalyst (CMIX-1, 5.0 mg) and the respective aryl bromide (5 mmol) in $HNiPr_2$ (10 mL) was carefully degassed (freeze and thaw) and was then heated to 80 °C with vigorous stirring for 5 min. After the addition of the respective acetylene (5.25 mmol), the precipitation of $HNiPr_2{\cdot}HBr$ indicated the start of the reaction and stirring was continued until full conversion was achieved (GC control). After cooling to room temperature, the reaction mixture was filtered and the precipitate washed with diethyl ether (25 mL). The volatiles were removed under vacuum and the residue was purified by flash column chromatography on silica (heptane or cyclohexane/ethyl acetate).

Acknowledgement

This work was supported by the TU Darmstadt and the DFG. We thank the Frankfurt Center for Scientific Computing for access to computer time.

[1] H. Doucet, J.-C. Hierso, *Angew. Chem.* **2007**, *119*, 850–888; *Angew. Chem. Int. Ed.* **2007**, *46*, 834–871.
[2] R. Chinchilla, C. Najera, *Chem. Rev.* **2007**, *107*, 874–922.
[3] E.-I. Negishi, L. Anastasia, *Chem. Rev.* **2003**, *103*, 1979–2017.
[4] M. Eckhardt, G. C. Fu, *J. Am. Chem. Soc.* **2003**, *125*, 13642–13643.
[5] C. A. Fleckenstein, H. Plenio, *Organometallics* **2007**, *26*, 2758–2767.
[6] J. Hillerich, H. Plenio, *Chem. Commun.* **2003**, 3024–3025.
[7] M. B. Thathagar, J. Beckers, G. Rothenberg, *Green Chem.* **2004**, *6*, 215–218.
[8] A. Köllhofer, H. Plenio, *Chem. Eur. J.* **2003**, *9*, 1416–1425.
[9] A. Köllhofer, T. Pullmann, H. Plenio, *Angew. Chem.* **2003**, *115*, 1086–1089; *Angew. Chem. Int. Ed.* **2003**, *42*, 1056–1058.
[10] A. Arques, D. Aunon, P. Molina, *Tetrahedron Lett.* **2004**, *45*, 4337–4340.
[11] D. A. Alonso, C. Najera, M. C. Pacheco, *Adv. Synth. Catal.* **2003**, *345*, 1146–1158.
[12] A. Köllhofer, H. Plenio, *Adv. Synth. Catal.* **2005**, *347*, 1295–1300.
[13] C. A. Fleckenstein, H. Plenio, *Chem. Eur. J.* **2007**, *13*, 2701–2716.
[14] H. Remmele, A. Köllhofer, H. Plenio, *Organometallics* **2003**, *22*, 4098–4103.
[15] A. Datta, H. Plenio, *Chem. Commun.* **2003**, 1504–1505.
[16] K. W. Anderson, S. L. Buchwald, *Angew. Chem.* **2005**, *117*, 6329–6333; *Angew. Chem. Int. Ed.* **2005**, *44*, 6173–6177.
[17] T. Ljungdahl, K. Pettersson, B. Albinsson, J. Martensson, *J. Org. Chem.* **2006**, *71*, 1677–1687.
[18] M. B. Thathagar, P. J. Kooyman, R. Boerleider, E. Jansen, C. J. Elsevier, G. Rothenberg, *Adv. Synth. Catal.* **2005**, *347*, 1965–1968.
[19] J.-C. Hierso, A. Fihri, R. Amardeil, P. Meunier, H. Doucet, M. Santelli, V. V. Ivanov, *Org. Lett.* **2004**, *6*, 3473–3476.
[20] C. S. Consorti, F. R. Flores, F. Rominger, J. Dupont, *Adv. Synth. Catal.* **2006**, *348*, 133–141.
[21] M. T. Rahman, T. Fukuyama, I. Ryu, K. Suzuki, K. Yonemura, P. F. Hughes, K. Nokihara, *J. Organomet. Chem.* **2006**, *691*, 2703–2706.
[22] E. A. B. Kantchev, C. J. O'Brien, M. G. Organ, *Angew. Chem.* **2007**, *119*, 2824–2870; *Angew. Chem. Int. Ed.* **2007**, *46*, 2768–2813.
[23] K. Königsberger, G.-P. Chen, R. R. Wu, M. J. Girgis, K. Prasad, O. Repic, T. J. Blacklock, *Org. Process Res. Dev.* **2003**, *7*, 733–742.
[24] S. Frigoli, C. Fuganti, L. Malpezzi, S. Serra, *Org. Process Res. Dev.* **2005**, *9*, 646–650.
[25] A. Zapf, M. Beller, *Top. Catal.* **2002**, *19*, 101–109.
[26] I.-B. Kim, B. Erdogan, J. N. Wilson, U. H. F. Bunz, *Chem. Eur. J.* **2004**, *10*, 6247–6262.
[27] H. Plenio, J. Hermann, A. Sehring, *Chem. Eur. J.* **2000**, *6*, 1820–1829.
[28] U. B. Vasconcelos, E. Dalmolin, A. A. Merlo, *Org. Lett.* **2005**, *7*, 1027–1030.
[29] H. Jude, D. J. Sinclair, N. Das, M. S. Sherburn, P. J. Stang, *J. Org. Chem.* **2006**, *71*, 4155–4163.
[30] U. Létinois-Halbes, P. Pale, S. Berger, *J. Org. Chem.* **2005**, *70*, 9185–9190.
[31] P. Vicennati, N. Bensel, A. Wagner, C. Créminon, F. Taran, *Angew. Chem.* **2005**, *117*, 7023–7026; *Angew. Chem. Int. Ed.* **2005**, *44*, 6863–6866.
[32] D. H. B. Ripin, D. E. Bourassa, T. Brandt, M. J. Castaldi, H. N. Frost, J. Hawkins, P. J. Johnson, S. S. Massett, K. Neumann, J. Phillips, J. W. Raggon, P. R. Rose, J. L. Rutherford, B. Sitter, A. M. Stewart, M. G. Vetelino, L. Wei, *Org. Process Res. Dev.* **2005**, *9*, 440–450.
[33] H. Meier, B. Mühling, H. Kolshorn, *Eur. J. Org. Chem.* **2004**, 1033–1042.
[34] R. G. Heidenreich, K. Köhler, J. G. E. Krauter, J. Pietsch, *Synlett* **2002**, 1118–1122.
[35] C. Yi, R. Hua, *J. Org. Chem.* **2006**, *71*, 2535–2537.
[36] H. Plenio, J. Hermann, J. Leukel, *Eur. J. Inorg. Chem.* **1998**, 2063–2069.
[37] R. J. T. Houk, E. V. Anslyn, *New J. Chem.* **2007**, *31*, 729–731.
[38] M. Hauck, J. Schonhaber, A. J. Zucchero, K. I. Hardcastle, T. J. J. Muller, U. H. F. Bunz, *J. Org. Chem.* **2007**, *72*, 6714–6725.
[39] C. Amatore, S. Bensalem, S. Ghalem, A. Jutand, Y. Medjour, *Eur. J. Org. Chem.* **2004**, 366–371.

 © 2008 Wiley-VCH Verlag GmbH & Co. KGaA, Weinheim

[40] A. Tougerti, S. Negri, A. Jutand, *Chem. Eur. J.* **2007**, *13*, 666–676.
[41] J. G. deVries, *Dalton Trans.* **2006**, 421–429.
[42] A. Jutand, *Eur. J. Inorg. Chem.* **2003**, 2017–2040.
[43] T. Rosner, J. L. Bars, A. Pfaltz, D. G. Blackmond, *J. Am. Chem. Soc.* **2001**, *123*, 1848–1855.
[44] A. A. C. Braga, N. H. Morgon, G. Ujaque, F. Maseras, *J. Am. Chem. Soc.* **2005**, *127*, 9298–9307.
[45] S. Shekhar, P. Ryberg, J. F. Hartwig, J. S. Mathew, D. G. Blackmond, E. R. Strieter, S. L. Buchwald, *J. Am. Chem. Soc.* **2006**, *128*, 3584–3591.
[46] A. A. C. Braga, G. Ujaque, F. Maseras, *Organometallics* **2006**, *25*, 3647–3665.
[47] U. Christmann, R. Vilar, *Angew. Chem.* **2005**, *117*, 370–378; *Angew. Chem. Int. Ed.* **2005**, *44*, 366–374.
[48] F. Barrios-Landeros, J. F. Hartwig, *J. Am. Chem. Soc.* **2005**, *127*, 6944–6945.
[49] J. F. Hartwig, *Inorg. Chem.* **2007**, *46*, 1936–1947.
[50] A. Nova, G. Ujaque, F. Maseras, A. Lledós, P. Espinet, *J. Am. Chem. Soc.* **2006**, *128*, 14571–14578.
[51] I. D. Hills, G. C. Fu, *J. Am. Chem. Soc.* **2004**, *126*, 13178–13179.
[52] I. P. Beletskaya, A. V. Cheprakov, *Chem. Rev.* **2000**, *100*, 3009–3066.
[53] S. Kozuch, S. Shaik, *J. Am. Chem. Soc.* **2006**, *128*, 3355–3365.
[54] X. Gao, H. B. Kagan, *Chirality* **1998**, *10*, 120–124.
[55] T. Satyanarayana, H. B. Kagan, *Adv. Synth. Catal.* **2005**, *347*, 737–748.
[56] O. Lavastre, R. Touzani, S. Garbacia, *Adv. Synth. Catal.* **2003**, *345*, 974–977.
[57] I. J. S. Fairlamb, A. R. Kapdi, A. F. Lee, *Org. Lett.* **2004**, *6*, 4435–4438.
[58] I. J. S. Fairlamb, A. R. Kapdi, A. F. Lee, G. P. McGlacken, F. Weissburger, A. H. M. deVries, L. S.-v. d. Vondervoort, *Chem. Eur. J.* **2006**, *12*, 8750–8761.
[59] I. J. S. Fairlamb, A. F. Lee, *Organometallics* **2007**, *26*, 4087–4089.
[60] J. G. deVries, L. Lefort, *Chem. Eur. J.* **2006**, *12*, 4722–4734.
[61] P. Chen, *Angew. Chem.* **2003**, *115*, 2938–2954; *Angew. Chem. Int. Ed.* **2003**, *42*, 2832–2847.
[62] M. T. Reetz, *Angew. Chem.* **2001**, *113*, 292–310; *Angew. Chem. Int. Ed.* **2001**, *40*, 284–310.
[63] C. Markert, A. Pfaltz, *Angew. Chem.* **2004**, *116*, 2552–2554; *Angew. Chem. Int. Ed.* **2004**, *43*, 2498–2500.
[64] T. Schareina, R. Kempe, *Angew. Chem.* **2002**, *114*, 1591–1594; *Angew. Chem. Int. Ed.* **2002**, *41*, 1521–1523.
[65] This estimate of this value is based on the accuracy of the determination of yields by gas chromatography. A 30% conversion represents the upper limit (initial rates), whereas a 0.3% conversion is the lowest conversion which can be determined with sufficient precision.
[66] M. an der Heiden, H. Plenio, *Chem. Commun.* **2007**, 972–974.
[67] J.-Y. Lee, G. C. Fu, *J. Am. Chem. Soc.* **2003**, *125*, 5616–5617.
[68] A. Tewari, M. Hein, A. Zapf, M. Beller, *Synthesis* **2004**, *8*, 935–941.
[69] G. Y. Li, *Angew. Chem.* **2001**, *113*, 1561–1564; *Angew. Chem. Int. Ed.* **2001**, *40*, 1513–1516.
[70] K. H. Shaughnessy, P. Kim, J. F. Hartwig, *J. Am. Chem. Soc.* **1999**, *121*, 2123–2132.
[71] C. A. Tolman, *Chem. Rev.* **1977**, *77*, 313–348.
[72] R. B. DeVasher, J. M. Spruell, D. A. Dixon, G. A. Broker, S. T. Griffin, R. D. Rogers, K. H. Shaughnessy, *Organometallics* **2005**, *24*, 962–971.
[73] D. White, B. C. Taverner, P. G. L. Leach, N. J. Coville, *J. Comput. Chem.* **1993**, *14*, 1042–1049.
[74] I. A. Guzei, M. Wendt, *J. Chem. Soc. Dalton Trans.* **2006**, 3991–3999.
[75] T. Kourti in *Design and Analysis in Chemical Research: Optimisation and Control*, (Ed.: R. L. Tranter), CRC Press, Boca Raton, **2000**.
[76] C. Hansch, A. Leo, R. W. Taft, *Chem. Rev.* **1991**, *91*, 165–195.
[77] S. Ehrenson, R. T. C. Brownlee, R. W. Taft, *Prog. Phys. Org. Chem.* **1973**, *10*, 1–80.
[78] H. Weissman, D. Milstein, *Chem. Commun.* **1999**, 1901–1902.
[79] D. Zim, V. R. Lando, J. Dupont, A. L. Monteiro, *Org. Lett.* **2001**, *3*, 3049–3051.
[80] L.-C. Liang, P.-S. Chien, M.-H. Huang, *Organometallics* **2005**, *24*, 353–357.
[81] R. Benhaddou, S. Czernecki, G. Ville, A. Zegar, *Organometallics* **1988**, *7*, 2435–2439.
[82] C. S. Consorti, M. L. Zanini, S. Leal, G. Ebeling, J. Dupont, *Org. Lett.* **2003**, *5*, 983–986.
[83] P. Fristrup, S. L. Quement, D. Tanner, P.-O. Norrby, *Organometallics* **2004**, *23*, 6160–6165.
[84] M. Ohff, A. Ohff, M. E. vanderBoom, D. Milstein, *J. Am. Chem. Soc.* **1997**, *119*, 11687–11688.
[85] V. P. W. Böhm, W. A. Herrmann, *Chem. Eur. J.* **2001**, *7*, 4191–4197.
[86] A. Brennführer, H. Neumann, S. Klaus, T. Riermeier, J. Almena, M. Beller, *Tetrahedron* **2007**, *63*, 6252–6258.
[87] nBu$_3$P was omitted from Figure 3 due to the extremely low activity of the Pd complex and the poor correlation coefficient of the linear fit.
[88] E. Galardon, S. Ramdeehul, J. M. Brown, A. Cowley, K. K. Hii, A. Jutand, *Angew. Chem.* **2002**, *114*, 1838–1839–1843; *Angew. Chem. Int. Ed.* **2002**, *41*, 1760–1763.
[89] A. Streitwieser, C. H. Heathcock, E. M. Kosover, *Organische Chemie*, VCH, Weinheim, **1994**.
[90] A. H. Roy, J. F. Hartwig, *J. Am. Chem. Soc.* **2003**, *125*, 13944–13945.
[91] M. Portnoy, D. Milstein, *Organometallics* **1993**, *12*, 1665–1673.
[92] S. Kozuch, C. Amatore, A. Jutand, S. Shaik, *Organometallics* **2005**, *24*, 2319–2330.
[93] T. R. Cundari, J. Deng, *J. Phys. Org. Chem.* **2005**, *18*, 417–425.
[94] A. Ariafard, Z. Lin, *Organometallics* **2006**, *25*, 4030–4033.
[95] I. D. Hills, M. R. Netherton, G. C. Fu, *Angew. Chem.* **2003**, *115*,5927–5930; *Angew. Chem. Int. Ed.* **2003**, *42*, 5749–5752.
[96] C. S. Consorti, F. R. Flores, J. Dupont, *J. Am. Chem. Soc.* **2005**, *127*, 12054–12065.
[97] C. Amatore, F. Pflüger, *Organometallics* **1990**, *9*, 2276–2282.
[98] J.-F. Fauvarque, F. Pflüger, M. Troupel, *J. Organomet. Chem.* **1981**, *208*, 419–427.
[99] L. J. Goossen, D. Koley, H. L. Hermann, W. Thiel, *Organometallics* **2005**, *24*, 2398–2410.
[100] J. Cioslowski, G. Liu, D. Moncrieff, *J. Phys. Chem. A* **1997**, *101*, 957–960.
[101] H. M. Senn, T. Ziegler, *Organometallics* **2004**, *23*, 2980–2988.
[102] A. D. Becke, *Phys. Rev. A* **1988**, *38*, 3098–3100.
[103] A. D. Becke, *J. Chem. Phys.* **1993**, *98*, 5648–5652.
[104] B. Miehlich, A. Savin, H. Stoll, H. Preuss, *Chem. Phys. Lett.* **1989**, *157*, 200–206.
[105] C. Lee, W. Yang, R. G. Parr, *Phys. Rev. B* **1988**, *37*, 785–789.
[106] R. Krishnan, J. S. Binkley, R. Seeger, J. A. Pople, *J. Chem. Phys.* **1980**, *72*, 650–654.
[107] A. D. McLean, G. S. Chandler, *J. Chem. Phys.* **1980**, *72*, 5369–5648.
[108] W. R. Wadt, P. J. Hay, *J. Chem. Phys.* **1985**, *82*, 284–298.
[109] However, there appears to be a relationship between some of the computed C–X bond energies and the experimental $\Delta H^{\ddagger}$ for the bond energies derived from reaction II, rather than for those obtained from reaction I.
[110] S. Kromidas, *Handbuch Validierung in der Analytik*, Wiley-VCH, Weinheim, **2000**.

Received: September 7, 2007
Revised: October 5, 2007
Published online: February 20, 2008

 © 2008 Wiley-VCH Verlag GmbH & Co. KGaA, Weinheim